Russian Physics Journal, Vol. 55, No. 2, July, 2012 (Russian Original No. 2, February, 2012)

PHYSICS OF SEMICONDUCTORS AND DIELECTRICS

INFLUENCE OF THE BACK CONTACT ON THE ELECTROPHYSICAL AND FUNCTIONAL CHARACTERISTICS OF THIN-FILM CdTe SCHOTTKY BARRIER DETECTOR STRUCTURES

Sh. A. Mirsagatov, A. S. Achilov, B. N. Zaveryukhin, and M. S. Baiev UDC 621. 315. 592

To register nuclear radiation, thin-film CdTe *Schottky barrier detector structures are developed. The structures are based on large-block p-*CdTe *films with resistivity* $\rho = 10^5 – 10^7$ Ω·*cm. The capacitance-voltage, current-voltage, amplitude, and noise characteristics of the structures are measured, and the mechanisms of charge carrier transfer are identified for different bias voltages. It is established that the functional characteristics of the detector structures are limited by the injection processes arising in the back* Mo *contact. It is found that the source of electron injection is the* MoO_3 *compound localized between the film and the molybdenum substrate.*

Keywords: films, cadmium telluride, detector, Schottky barrier, back contact, injection, noise.

INTRODUCTION

Cadmium telluride (CdTe) is widely used to develop x-ray and γ-ray detectors. Large atomic numbers of the components of this material and the gap width provide higher efficiency of nuclear radiation detection by CdTe detectors without cooling compared to Si and Ge detectors. Single-crystal CdTe and $Cd_{1-x}Zn_xTe$ detectors have already demonstrated theirs advantages over the Si and GaAs detectors and are successfully used in x-ray and γ-ray spectrometry. In recent years, detectors based on CdTe and $Cd_{1-x}Zn_xTe$Schottky barrier materials have been developed intensively [1–3]. Significant advantages of these detectors are low dark reverse currents (~10^{-7} A) and high working temperatures ($T \geq 300$ K). In addition, the Schottky barrier diode detectors can register photons with energies up to 1 MeV and higher with ultimate energy resolution [4]. It is well known that single crystals of A^2B^6 compounds used to produce nuclear radiation detectors have some disadvantages. The main disadvantage of the A^2B^6 single crystals is the presence of significant number of defects of different nature that reduce the lifetime of charge carriers and worsen the detector characteristics [5]. These disadvantages can be eliminated if the large-block polycrystalline CdTe films with columnar grain structure (crystallites) are used as a base material. In such films, grains occupy the entire film thickness. The advantage of these polycrystalline films is that they have the properties of single crystals in the direction of theirs growth and the properties of polycrystals in the horizontal direction. The grain boundaries serve as sinks for defects of various types, thereby leading to an increase in the lifetime of charge carriers in the crystallites [6]. On the other hand, these boundaries can shunt the crystallites and serve as main sources of leakage currents. Therefore, passivation of grain boundaries is of paramount importance for polycrystalline semiconductor materials used to make solid-state electronic devices. In this direction, we have developed the technology that allows us to grow large-block polycrystalline CdTe

Physical-Technical Institute of the Scientific-Production Association "Physics-Sun" of the Academy of Sciences of the Republic of Uzbekistan, Tashkent, Republic of Uzbekistan, e-mail: mirsagatov@rambler.ru. Translated from Izvestiya Vysshikh Uchebnykh Zavedenii, Fizika, No. 1, pp. 47–52, January, 2012. Original article submitted October 20, 2010; revision submitted May 24, 2011.

 1064-8887/12/5502-0180

films with different resistivities ρ, different thicknesses, and sufficiently long lifetimes of minority carriers ($\tau \sim 10^{-7}$–10^{-6} s for $\rho \approx 10^7$ Ω·cm).

We have already produced thin-film CdTe detectors based on the metal–oxide–semiconductor structures [7]. These detectors demonstrated high efficiency of x-ray registration.

The aim of this work is to develop and produce a thin-film structure for CdTe Schottky barrier detector of new type and to elucidate reasons for noise increase and limitations on the improvement of the spectrometric characteristics (SC). The existence of the barrier allowed us to investigate the influence of near-contact regions of the back Mo contact on the characteristics of thin-film CdTe detector structures.

SAMPLES

Thin-film CdTe detector structures were produced by aluminum deposition on the surface of *p*-type large-block CdTe films in vacuum ($P \sim 10^{-5}$ Torr). The back contact was made of the molybdenum plate with thickness of 300 μm, because there is a good adhesion between this contact and the *p*-CdTe films. We prepared the structures of types *a* and *b*. In the structures of type *a*, there was no MoO_3 layer between the *p*-CdTe films and Mo contacts, and the detectors based on these structures had high spectrometric characteristics [7]. In detectors based on the structures of type *b*, the MoO_3 layer existed between the *p*-CdTe film and the Mo contact formed in the process of *p*-CdTe film growth on the Mo substrate. It was then established that the detectors of this type had the worst performance characteristics compared to the detectors of type *a*. Therefore, it was interesting: a) to examine the effect of the near-contact regions with MoO_3 layers and the degree of compensation on the expansion of the space charge region, carrier transfer in CdTe detectors with MoO_3 layers, and the detector characteristics, and b) to determine optimal working bias voltages at which high spectral characteristics are achieved. In the detectors of both types, the *p*-CdTe films had the resistivity $\rho \approx 10^5$–10^7 Ω·cm and the minority carrier lifetime of the order of 10^{-7}–10^{-6} s. The films had the columnar grain structure and practically the single crystal structure in the growth direction. The transverse grain sizes ranged from 100 to 150 μm. The thickness of the *p*-CdTe films was $L \approx 30$–50 μm, so that grains occupied the entire film thickness. The detector *p*-CdTe films were compensated materials and were formed on the Mo substrates.

In the detectors with MoO_3 layers, the nonequilibrium charge carriers were generated by α-particles with energy $E = 5.150$ MeV emitted from a Pu^{239} source. In our experiments, we measured the dependence of the signal amplitude (M) of the detectors on the reverse bias voltage V_R – $M(V_R)$. This allowed us to analyze the processes of nonequilibrium carrier transfer as functions of the degree of compensation of the *p*-CdTe films, that is, of the film resistivity. We also studied the behavior of the capacitance, current, and detector noise with the reverse bias voltage V_R (a negative potential was applied to the Mo substrate).

EXPERIMENTAL RESULTS AND DISCUSSION

The capacitance-voltage characteristic $C(V)$ of the Al–*p*-CdTe–Mo detector structure (*p*-CdTe films had $\rho \approx 10^7$ Ω·cm) is shown in Fig. 1 in the conventional coordinates $1/C^2 = f(V_R)$ at AC signal frequency $f = 100$ kHz. The increasing section of this characteristic shows a bent and consists of two straight lines *1* and *2*, respectively. The presence of straight lines *1* and *2* indicates inhomogeneity of the near-surface *p*-CdTe layer. The effective impurity concentrations N_{eff} calculated from these two straight lines that describe dependences of C^{-2} on V_R were $1.2 \cdot 10^{12}$ and $3.1 \cdot 10^{12}$ cm^{-3}, respectively. The characteristic $C(V)$ reaches a plateau at bias voltages $V_R \sim 3$–4 V. This means that at these voltages, the space charge occupied the entire thickness of the base of the Al–*p*-CdTe–Mo structure. In the plateau of the $C(V)$ characteristic, the detector capacitance is $C \approx 12.2$ pF. Evaluation of the space charge layer thickness d using the well-known formula for the plane capacitor gives $d \sim 45.7$ μm for $\varepsilon = 9$ [8], $\varepsilon_0 = 8.85 \cdot 10^{-14}$ F·cm^{-1} (here ε and ε_0 are the dielectric constants of the semiconductor and vacuum, respectively), and the detector structure area $S \approx 7 \cdot 10^{-2}$ cm^2, which practically corresponds to the *p*-CdTe film thickness $L = 46$ μm.

In this structure, the capacitance is $C = 16.8$ pF and the space charge layer thickness is $d \sim 33$ μm at $V_R = 0$. The mean free path of the *α*-particles $R \approx 25$ μm falls completely within this space charge layer.

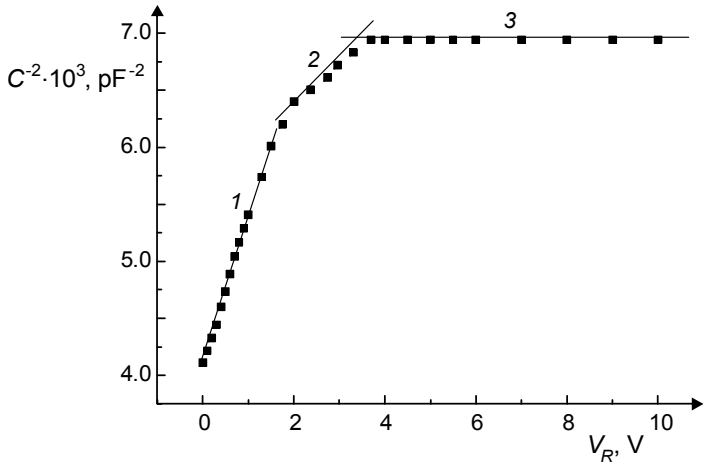

Fig. 1. Capacitance-voltage characteristic of CdTe Schottky barrier detector structure No. 12 in the coordinates $C^{-2}(V)$ for test signal frequency f = 100 kHz, T = 293 K, and resistivity of the structure base $\rho \approx 10^7$ Ω·cm.

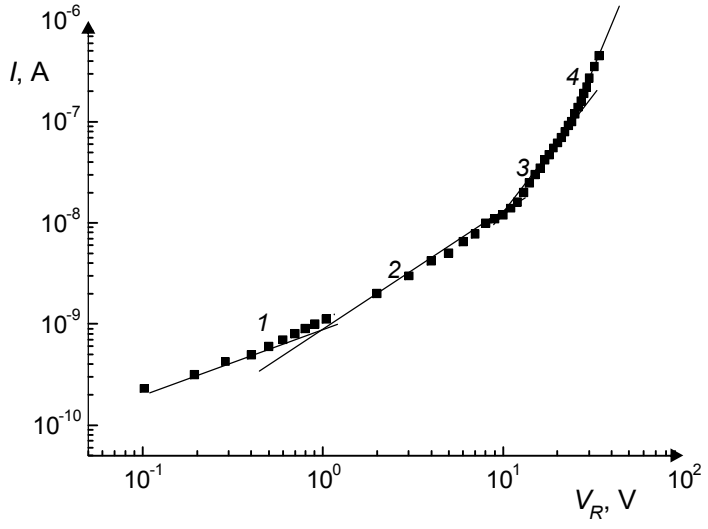

Fig. 2. Capacitance-voltage characteristic of CdTe Schottky barrier detector structure No. 12 drawn on the log-log scale for T = 293 K and resistivity of the structure base $\rho \approx 10^7$ Ω·cm.

The current-voltage characteristic (CVC) of the CdTe Schottky barrier detector is described by the following expression for the current: $I = A \cdot V^{\alpha}$ (where α is a dimensionless coefficient) and comprises four sections (Fig. 2): $I = A \cdot V^{\alpha_1}$ for $\alpha_1 \approx 0.55$ (section *1*), $I = A \cdot V^{\alpha_2}$ for $\alpha_2 \approx 1$ (section *2*), $I = A \cdot V^{\alpha_3}$ for $\alpha_3 \approx 2$ (section *3*), and $I = A \cdot V^{\alpha_4}$ for $\alpha_4 \approx 3.9$ (section *4*). In the first section of the CVC, the current is limited by that generated in the space charge layer, since it is well described by the formula [8]

$$I_r = \frac{n_i}{2\tau_0}\left(\frac{2q\varepsilon\varepsilon_0}{N_{A,\text{eff}}}\right)^{\frac{1}{2}} \varphi_k - \frac{n_i}{2\tau_0}\left(\frac{2q\varepsilon\varepsilon_0}{N_{A,\text{eff}}}\right)^{\frac{1}{2}} V^{\frac{1}{2}}, \quad (1)$$

where n_i is the intrinsic concentration of charge carriers, q is the electron charge, $N_{A,\text{eff}}$ is the effective concentration of charged acceptor centers, φ_k is the contact potential difference, and $\tau_0 = \tau_n = \tau_p$ is the lifetime of charge carriers in the intrinsic semiconductor.

From the slope of straight line *1* (Fig. 2), the carrier lifetime $\tau_0 \approx 5 \cdot 10^{-7}$s was calculated using formula (1) with the following parameter values: intrinsic carrier concentration in CdTe of cubic modification $n_i \approx 10^6$ cm^{-3} at $T = 293$ K, $\varepsilon = 9$, $\varepsilon_0 = 8.85 \cdot 10^{-14}$ F/cm, $S = 0.07$ cm^2, and $N_{A,\text{eff}} = 2.1 \cdot 10^{12}$ cm^{-3}. For $N_{A,\text{eff}} = 3.5 \cdot 10^{12}$ cm^{-3}, $\tau_0 \sim 3.3 \cdot 10^{-7}$ s. For Schottky barrier detectors based on *p*-CdTe-films with $\rho \approx 10^5$ Ω·cm, the carrier lifetime was $\tau_0 \sim 4 \cdot 10^{-8}$ s.

It follows from these data that the lifetime of charge carriers increases with ρ of the base. It is well known that an increase in the resistivity of cadmium telluride films is due to the increased synthesis temperature at which the probability of production and accumulation of free tellurium (Te) atoms on the crystallite surface increases [9]. The tellurium atoms easily form the TeO_2 compound, which is a good dielectric. This dielectric contributes to passivation of the grain boundaries. As a result of passivation, the concentration of the surface states decreases, and the carrier lifetime increases.

Let us consider the second CVC section where the current-voltage behavior is described by a linear dependence. From this CVC section, we calculated that $\rho \approx 4 \cdot 10^{10}$ Ω·cm for $L = 46$ μm and $S = 0.07$ cm^2 (the area of the upper Al contact). This ρ value is almost the same as the resistivity of the cubic modification of cadmium telluride with intrinsic conductivity. This confirms that the space charge occupies the entire thickness of the *p*-CdTe film.

The quadratic dependence of the current on voltage (section *3* of the *I–V* characteristic) is due to unipolar injection of electrons from the back contact. The results of x-ray phase analysis demonstrated and confirmed that the MoO_3 oxide layer was formed between the *p*-CdTe film and the Mo substrate. This layer, being the *n*-type semiconductor, was the source of unipolar injection. The dielectric relaxation time was estimated from the formula $t_\Omega \approx 10^{-12}\rho$ [8]. The effective mobility (μ_{eff}) estimated from the voltage V_x at which transition from Ohm's law to the quadratic law was observed for the CVC [9] and the slope of the quadratic section of the current-voltage characteristic were $\mu_{\text{eff}} \approx 3.4 \cdot 10^{-3}$ and $\approx 4.4 \cdot 10^{-3}$ cm$^2 \cdot$V$^{-1} \cdot$s^{-1}, respectively. This fact demonstrates that the space charge is formed in the detector structure. Thus, the current transfer mechanism in the structure under study is determined by the unipolar injection. These results also confirm that the majority of injected electrons are localized in shallow traps.

Let us now analyze the fourth CVC section where $I = AV^{3.9}$. This section of the sharp current increase is observed for unipolar injection when the adhesion level is intersected with the Fermi quasi-level or these levels are very close [10]. The calculated concentration of unoccupied traps was $p_{t,0} \approx 10^{15}$ cm^{-3}. The ratio of concentrations of unoccupied traps and nonequilibrium free electrons $\frac{p_{t,0}}{n} \approx 145$ demonstrates that the nonequilibrium concentration of free electrons is $n \approx 10^{13}$ cm^{-3}. Hence it follows that the n value is more than two orders of magnitude smaller than the unoccupied trap center concentration.

We now analyze the dependence of the detector noise E_n on the bias voltage V_R (Fig. 3). As can be seen from Fig. 3, the noise of the detector structure reaches a minimum value $E_\text{n} \sim 16$ keV at $V_R = 4$ V and remains constant up to $\sim V_R = 8$ V. Then it starts to increase again. A comparison of the dependence $E_\text{n}(V_R)$ with the capacitance-voltage characteristic demonstrates that the noise reaches a minimum value at the voltage at which the space charge completely occupies the entire thickness of the detector base (*p*-CdTe layer). This bias voltage is optimal. As demonstrated below, the spectral V_R characteristics are improved in this case. For these values of V_R, the region where the dependence $E_\text{n}(V_R)$ is constant corresponds to the linear CVC section. Recall that the ρ value calculated from the linear section of the current-voltage characteristic corresponds to the intrinsic resistivity of cadmium telluride with cubic modification. This means that at minimal noise value, no electrons are injected or their concentration is much lower than n_i, that is, $n_i > n$. It should be noted that the voltage V_x at which the transition from Ohm's law to the quadratic law is observed for the CVC coincides with the V_R value at which the noise of the detector structure starts to increase. If we consider that at V_x, the concentration of injected electrons n is twice greater than n_i and the space charge is formed in the base, it becomes apparent that electrons injected from the back contact area serve as main sources of noise.

Then we consider the dependence of the signal amplitude $M(V_R)$ on the applied bias voltage when registering α-particles (Figs. 4 and 5). As seen from Fig. 4, the dependence $M(V_R)$ has four sections. The onset of the first section of this dependence corresponds to the voltage at which the base thickness is completely occupied by the space charge.

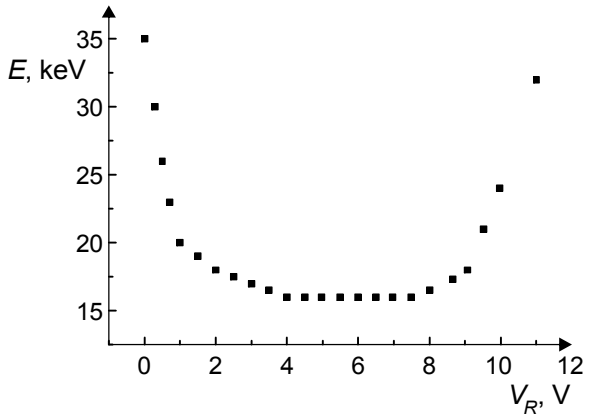

Fig. 3. Dependence of noise on the bias voltage of CdTe structure No. 12 at $T = 293$ K. The resistivity of the structure base was $\rho \approx 10^7$ Ω·cm.

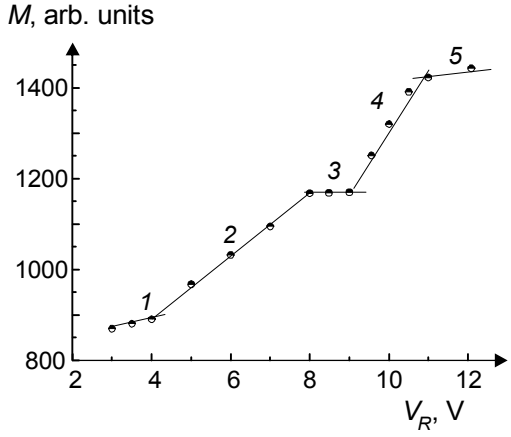

Fig. 4

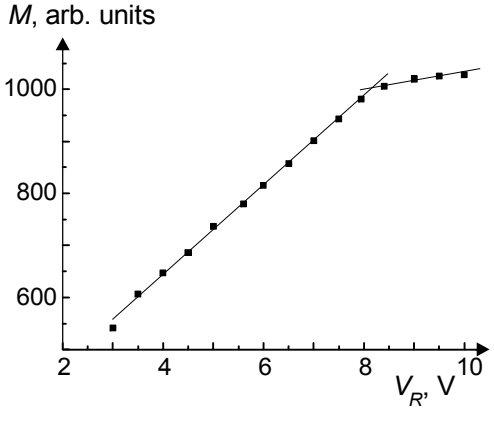

Fig. 5

Fig. 4. Dependence of the signal amplitude of CdTe detector structure No. 12 on the reverse bias voltage at $T = 293$ K. The resistivity of the structure base was $\rho \approx 10^7$ Ω·cm.

Fig. 5. Dependence of the signal amplitude of detector CdTe structure No. 21 on the reverse bias voltage at $T = 293$ K. The resistivity of the structure base was $\rho \approx 10^5$ Ω·cm.

Therefore, further increase in the bias voltage on the detector structure leads only to an increase in the electric field strength in the space charge layer, which contributes to a more efficient collection of nonequilibrium charge carriers created by α-particles.

This section continues up to $V_R = 8$ V, where the space charge created by electrons injected from the region of the Mo contact appears (Fig. 2, intersection point of straight lines *2* and *3*). In the voltage range $V_R = 8$–9 V, the signal amplitude remains practically constant. Under these bias voltages, the space charge enters directly the surface of the intermediate MoO_3 layer between CdTe and Mo. This intermediate layer is inhomogeneous and has a complex composition. Microinhomogeneities (accumulated impurities, structural defects, etc.) on the surface of this layer capture nonequilibrium carriers, thereby leading to the appearance of section *3* in the $M(V_R)$ dependence (Fig. 4). Further increase in the electric field strength in the space charge layer does not lead to capture of drifting charge carriers, since these traps have been filled completely. Therefore, an increase in the signal amplitude in the voltage range $V_R = 9$–11 V

is due to an increase in the drift velocity of nonequilibrium carriers, which decreases the probability of their capture by traps. In so doing, the field-induced ejection of carriers previously captured by deep traps cannot be excluded [11].

An analysis of the current-voltage characteristic (Fig. 2) demonstrates that starting with V_R = 11 V, the rapid current growth is observed due to electron injection from the near-contact region of the Mo-contact, that is, from the MoO_3 layer. At the same value V_R = 11 V, a sharp increase in the noise of the detector structure is observed (Fig. 3).

We also investigated the characteristics of detectors based on *p*-CdTe films with different values of ρ. For example, for the detector with the base layer which had ρ ≈ 10^5 Ω·cm, the signal amplitude increased linearly in the range V_R = 3–8 V and then reached the plateau (Fig. 5). For such detector structures with low ρ value of the base, the voltage V_R at the beginning of the plateau in the $M(V_R)$ dependence coincided with the V_R value in the current-voltage characteristic. At these V_R values, a sharp increase in the current began due to injection of electrons from the near-contact region of the back contact, thereby leading to an increase in the noise of the detector structure and worsening the efficiency of radiation detection. In the detector structures with low ρ value of the base, the space charge had no time to occupy the entire thickness of the base due to electron injection from the MoO_3 layer.

CONCLUSIONS

The Schottky barrier detector structures have been developed based on the large-block *p*-CdTe films with resistivity ρ = 10^5–10^7 Ω·cm. It was demonstrated that at low bias voltages, the mechanism of current transfer in these structures was determined by generation of thermal carriers in the space charge layer.

At large bias voltages, mainly electrons injected from the contact region, that is, from the MoO_3 layer to the base of the structure contributed to the current transfer mechanism and noise characteristics, which worsened the efficiency of radiation detection.

It was established that the ranges of small and large bias voltages as well as the lifetime of nonequilibrium charge carriers were directly dependent on the ρ value of the base. The optimal working range of the bias voltage was determined for the detector structures with Mo back contacts.

It was demonstrated that the source of electron injection was the MoO_3 compound located between the *p*-CdTe film and the molybdenum substrate.

REFERENCES

1. T. Takahashi and S. Watanabe, IEEE Trans. Nucl. Sci., **48**, 950 (2001).
2. S. Watanabe, T. Takahashi, Y. Okada, *et al*., IEEE Trans. Nucl. Sci., **49**, 210 (2002).
3. T. Tanaka, T. Kabayashi, T. Mitani, *et al*., New Astron. Rev., **48**, (2004) 309.
4. L. A. Kosyachenko, V. M. Sklyarchuk, O. L. Maslyanchuk, *et al*., Pis'ma Zh. Tekh. Fiz., **32**, No. 24, 29–37 (2006).
5. H. Hermon, M. Shieber, and R. B. James, J. Electron. Mater., **28**, 688–702 (1999).
6. G. Harbeke, ed., Polycrystalline Semiconductors [Russian translation], Mir, Moscow (1989).
7. B. N. Zaveryukhin, Sh. A. Mirsagatov, *et al*., Pis'ma Zh. Tekh. Fiz., **29**, No. 22, 80–87 (2003).
8. I. M. Vikulin and V. I. Stafeev, Physics of Semiconductor Devices [in Russian], Sovetskoe Radio, Moscow (1980).
9. K. Zanio, Semiconductors and Semimals, Vol. 13, Academic Press, New York (1978).
10. M. A. Lampert and P. Mark, Current Injection in Solids [Russian translation], Mir, Moscow (1973).
11. V. K. Eremin, N. B. Strokan, and N. I. Tisnek, Fiz. Tekh. Poluprovodn., **9**, No. 8, 1575–1579 (1975).